

SURFACE REACTION MECHANISM AND LEPTON SCREENING FOR COLD FUSION WITH ELECTROLYSIS

Yeong E. Kim

Department of Physics, Purdue University
West Lafayette, IN 47907

ABSTRACT

A surface reaction mechanism and the effects of electron and muon screening are described for electrolysis fusion experiments. A general expression is given for the modified Coulomb barrier penetration factor which includes the lepton screening effect and which can be used for extrapolating the fusion cross sections to lower energies. It is shown that, when combined with the effect of velocity distribution in the context of the surface reaction mechanism, the electron screening effect may explain the claimed results of recent electrolysis fusion experiments and may also explain why it is difficult to reproduce the same result with different samples in electrolysis experiments. Experimental tests of the effects of electron and muon screening are suggested both for electrolysis experiments and for inelastic scattering experiments.

I. INTRODUCTION

Recently, a surface reaction mechanism [1,2] was proposed for electrolysis fusion experiments [3-8] in which deuterium-deuterium (D-D) fusion takes place in the surface zone of a palladium (Pd) cathode where whiskers and asperities of metal deuterides form during the electrolysis experiments, in order to explain the discrepancy of 24-60 orders of magnitude between the conventional estimates [9-10] and the electrolysis fusion results [3-8]. It has been shown that the calculated fusion reaction rate can increase by as much as 60 orders of magnitude [11] if an appropriate Maxwell-Boltzmann velocity distribution is used in the context of the proposed surface reaction mechanism.[1,2] It has also been argued that

the conventional theoretical estimates of the cold D-D fusion rate may not be reliable since the extrapolation method used may not be valid at low energies.[1,2,12]

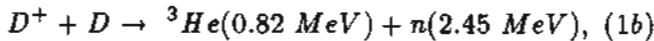
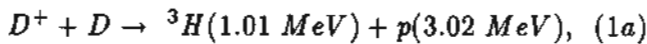
In this paper, it is shown that the electron screening effect becomes significant at low energies and hence the conventional Coulomb barrier penetration factor (the "Gamow" factor) used to describe the D-D fusion rate is no longer valid at low energies. A modified Coulomb barrier penetration factor and a new extrapolation method for the cross-section and rate are proposed for the cold D-D fusion reaction in electrolysis experiments and for other fusion reactions in physical processes. When combined with an appropriate velocity distribution arising from the surface reaction mechanism, the new extrapolation formula which includes the electron screening effect is expected to be able to explain the results [3-8] of electrolysis fusion experiments.

In section II, the D-D and hydrogen-deuterium (H-D) fusion reactions are described in terms of the surface reaction mechanism. In section III, the effect of a velocity distribution on D-D fusion is discussed in the context of the surface reaction mechanism. In section IV, the electron screening effect is described in detail for fusion reactions and an appropriate modification of the Coulomb barrier penetration factor is presented. A new extrapolation formula for the fusion cross sections is given. The physical consequences of the effects of both velocity distribution and electron screening are discussed for electrolysis fusion experiments. In section V, the muon screening effect is discussed and its implications are described for the results of the recent electrolysis experiments. In section VI, the branching ratio for the D-D fusion reactions is discussed. Finally, a brief summary is given in section VII.

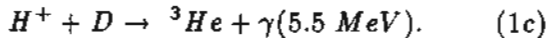
II. FUSION PROCESSES IN THE SURFACE ZONE

In electrolysis experiments where the Pd cathode is immersed in D_2O with $LiOD$ electrolyte, many spherical and hemispherical D_2 gas bubbles of varying sizes (radii ranging from a few μm to a few mm) will be produced continuously in the surface zone outside the Pd cathode where they will stay for a certain time duration before they move out of the electrolysis cell. Many of these D_2 gas bubbles in the surface zone will have surface whiskers (PdD or LiD) protruding into them. This will create very high electric fields around the sharp tips of the whiskers, which are many orders of magnitude larger than the average field due to the applied potential. D^+ ions in a given bubble will gain kinetic energies with a statistical distribution which depends on the bubble size and the values of the widely varying electric field inside the bubble. When the applied potential is ~ 10 V, the average laboratory kinetic energy of the D^+ ions in each bubble is expected to be ~ 10 eV. A small fraction of the D^+ ions are expected to gain additional kinetic energy beyond the average value due to several acceleration processes, such as (i) acceleration of the ion due to a change of the polarity of D^+ to D or D^- near the whisker tips (this process $D^+ \rightarrow D^-$ may increase the the D kinetic energy by a factor of two, or more by the use of a high AC voltage with a correct modulation frequency), (ii) acceleration of D when D^+ is picked up and carried by a group of fast electrons [13], and (iii) other such processes [13].

The accelerated D^+ ions (deuterons) (also smaller amounts of D^- and D) in the bubble will be incident on the electrically neutral D (or H present as an impurity) in the D_2O or in the Pd cathode (whiskers and surface areas). The dominant fusion reactions are:



and



Reaction (1c) is included since it has been recently shown that the H-D fusion cross-section and reaction rate are larger than those for reactions (1a) and (1b) for $E \leq 8eV$ in the center of mass (CM) frame [14] and is thus expected to compete with the D-D fusion below $E(CM) \approx 2.5$ eV for an impurity ratio of $H/D \approx 10^{-3}$ in electrolysis experiments. Experiment values of the cross-section, $\sigma(E)$, for (1a), (1b), and (1c) have been parameterized as [15]

$$\sigma(E) = \frac{S(E)}{E} e^{-(E_a/E)^{1/2}} \quad (2)$$

where E_G is the "Gamow energy" given by $E_G = (2\pi\alpha Z_D Z_D)^2 Mc^2/2$ or $E_G^{1/2} \approx 31.39(keV)^{1/2}$ for the reduced mass $M \approx M_D/2$ for reactions (1a) and (1b) and $E_G^{1/2} = 25.64(keV)^{1/2}$ for reaction (1c) with the reduced mass $M = m_p M_D/(m_p + M_D) \approx M_D/3$. E is in units of keV in the center of mass (CM) reference frame. The S-factor, $S(E)$, is extracted from the experimentally measured values [16,17] of the cross-section, $\sigma(E)$, for $E \gtrsim 4$ keV and is nearly constant [17], $S(E) \approx 52.9$ keV - b, for both reactions (1a) and (1b) in the energy range of interest here, $E \lesssim 1$ keV. For reaction (1c), $S(E) \approx 2.50 \times 10^{-4} keV - b$. In the following, the theoretical formulation will be given only for reactions (1a) and (1b), as it is similar for reaction (1c).

Reaction rates, R_{calc} , for both reactions (1a) and (1b) for an incident deuteron kinetic energy E_i in the laboratory (LAB) frame, are given by

$$R_{calc}(1a) = R_{calc}(1b) = \Phi P(E_i), \quad (3)$$

where Φ is the incident D^+ flux

$$\Phi = (0.625 \times 10^{19} D^+ 's/sec)I \quad (4)$$

with the current I in units of amperes, and $P(E_i)$ is the probability for a deuteron to undergo a fusion reaction (1a), (1b), or (1c) while slowing down in the deuterated Pd electrode, which can be written as

$$P(E_i) = \int dx n_D \sigma(E_{DD}) = \int_0^{E_i} dE_D \frac{1}{|dE_D/dx|} \sigma(E_{DD}) \quad (5)$$

E_D and E_{DD} are the deuteron kinetic energies in the LAB and CM frames, respectively ($E_{DD} = E_D/2$). The stopping power [18] for $E_D \lesssim 12$ keV is given by

$$\frac{dE_D}{dx} = 3.70 \times 10^{-15} n_{Pd} \sqrt{E_D} eV - cm^2 \quad (6)$$

for D in Pd and

$$\frac{dE_D}{dx} = 0.89 \times 10^{-15} n_D \sqrt{E_D} eV - cm^2 \quad (7)$$

for D in D. Therefore, the stopping power for D in PdD is given by the sum of eqs. (6) and (7),

$$\frac{dE_D}{dx} = 3.1 \times 10^5 \sqrt{E_D} keV/cm \quad (8)$$

for $n_{Pd} = 6.767 \times 10^{22} cm^{-3}$ and $n_D = n_{Pd}$. E_D in eq. (8) is in units of keV in the LAB frame.

With the given choice of parameterizations, eqs. (2) and (8), the integration in eq. (5) can be done

analytically to yield the following expression for eq. (3).

$$\begin{aligned} R_{calc}(1a) &= R_{calc}(1b) \\ &= 2.3 \times 10^{12} I \exp(-44.24/\sqrt{E_i}), \end{aligned} \quad (9)$$

with I in units of amperes and E_i in units of keV (LAB).

Calculations for $R_{calc}(1a)$, $R_{calc}(1b)$, and $R_{calc}(1c)$ for the case in which D^+ is incident on D (or H) in D_2O (or H_2O) can be carried out in the same way, but the results will not be given here.

The range $R(E_i)$ of D^+ in PdD can be obtained from eq. (8) as

$$R(E_i) = \int dx = \int_0^{E_i} \left(\frac{dE}{dx}\right)^{-1} dE$$

or

$$R(E_i) = 0.645 \times 10^{-6} \sqrt{E_i(\text{in keV})} \text{ cm} \quad (10)$$

which yields $R(E_i) = 2.04 \text{ \AA}$, 6.45 \AA , and 20.4 \AA for $E_i = 1 \text{ eV}$, 10 eV , and 100 keV , respectively. The range $R(E_i)$ of D^+ in D_2O is slightly larger than that of D^+ in PdD. Since individual D in Pd is separated by $\sim 2 \text{ \AA}$, D^+ penetrates into 2, 4, and 11 layers from the surface of PdD when the incident D^+ energies (LAB) are 1 eV, 10 eV, and 100 eV, respectively. Therefore, D-D fusion takes place within the first few surface layers of PdD and of D_2O surrounding the bubbles in electrolysis experiments.

III. THE EFFECT OF VELOCITY DISTRIBUTION

In order to compare with the experimental rates which are usually given in units of sec^{-1} per deuterium, the theoretical D-D fusion rate ($\text{sec}^{-1}/D - D \text{ pair}$), Λ_δ , is defined as

$$\Lambda_\delta = \frac{n_D}{2} \sigma(E) v(CM) \quad (11)$$

for a sharp (delta-function) velocity distribution where $E = E_{DD} = \frac{M}{2} v^2(CM) = \frac{M_D}{4} v^2(LAB) = \frac{1}{2} E_D(LAB)$ and $n_D \approx 6 \times 10^{22} \text{ cm}^{-3}$. The estimated values of $\Lambda_\delta(E)$ calculated from eqs. (2) and (11) for a sharp velocity distribution have been used to argue against the possibility of D-D fusion in electrolysis experiments. However, a statistical velocity distribution is more appropriate in electrolysis experiments as discussed in section II. It has been argued [1,2] and shown [11] that the D-D fusion rate with a Maxwell-Boltzmann D^+ velocity distribution can become very large at low energies compared to that with a sharp velocity distribution.

Since the precise form of the D^+ velocity distribution in electrolysis experiments is not known at present, we assume a Maxwell-Boltzmann distribution with and without a cut-off for high velocity components. The temperature term, $k_B T$, will be replaced by the "average" kinetic energy, E_{DD} , in the center of mass (CM) D-D frame, which is related to the most probable velocity $v(CM)$ by $E_{DD} = \frac{M}{2} v^2(CM)$ with the reduced mass $M = M_D/2$.

For a Maxwell-Boltzmann velocity distribution, the D-D fusion rate, $\Lambda(\text{sec}^{-1}/D - D \text{ pair})$, for reaction (1a) or (1b) is given by [15]

$$\Lambda(E_{DD}) = \frac{n_D}{2} \langle \sigma v \rangle, \quad (12)$$

with

$$\langle \sigma v \rangle = \frac{(8/\pi)^{1/2}}{M^{1/2}(E_{DD})^{3/2}} \int_0^{E_c} \sigma(E) E e^{-E/E_{DD}} dE, \quad (13)$$

where the cross-section, $\sigma(E)$, is parameterized (E is in the C.M. frame) by eq. (2) which is the conventional form assuming non-resonant charged particle reactions for reactions (1a) and (1b).

The D-D fusion rate for reaction (1a), $\Lambda_{exp}^T(1a) \approx 10^{-19} \text{ sec}^{-1}$, inferred by Fleischmann et al.[3] from the measurement of tritium production, and also the D-D fusion rate for reaction (1b), $\Lambda_{exp}^n(1b) \approx 10^{-23} \text{ sec}^{-1}$, obtained by Jones et al.[4] are often criticized as being impossible or incorrect when compared to estimates of Λ in bulk matter (an upper limit of $\Lambda \lesssim 10^{-47} \text{ sec}^{-1}$) [9] or to the result of Λ_δ obtained from eq. (11). Our recent results [11] for Λ calculated from eqs. (12) and (13) indicate that $\Lambda_{exp}^n(1b) \approx (10^{-23}/\text{sec})$ [4] and $\Lambda_{exp}^T(1a) \approx (10^{-19}/\text{sec})$ [3] are consistent with calculated values of $\Lambda(E_{DD}) \approx 10^{-23} \text{ sec}^{-1}$ and $\Lambda(E_{DD}) \approx 10^{-19} \text{ sec}^{-1}$ for $E_{DD} \approx 15 \text{ eV}$ and 20 eV , respectively. Therefore, the claimed values of $\Lambda_{exp}^n(1b) \approx (10^{-23}/\text{sec})$ [4] and $\Lambda_{exp}^T(1a) \approx (10^{-19}/\text{sec})$ [3] are physically acceptable values for the D-D fusion rate in electrolysis experiments if the applied potentials are 30V and 40V, respectively. To match the D-D fusion rate $\Lambda(E_{DD})$ of eq. (1a) to the rate, $\Lambda_{exp}^{heat}(1a) \approx (10^{-10}/\text{sec})$ [3], inferred by excess heat measurements [3,4,6], an "average" kinetic energy of $E_{DD} \approx 75 \text{ eV}$ is needed. In the following section, it will be shown that the above remaining discrepancies can be explained by the effect of electron screening.

IV. ELECTRON SCREENING EFFECT

The expression for $\sigma(E)$ given by eq. (2) is valid only for a reaction in which D^+ is incident on another D^+ . In electrolysis fusion experiments as well

as in other physical processes [14], D^+ (also D^- or D) is incident on D which is shielded by an electron cloud; i.e., the target D is electrically neutral outside the electron shielding radius ($\approx 0.53 \text{ \AA}$, the Bohr radius). Therefore, the Coulomb barrier penetration factor ("Gamow factor") in eq. (2)

$$P_G(E) = \exp(-(E_G/E)^{1/2}) \quad (14)$$

which is appropriate only for the ($D^+ + D^+$) reaction has to be modified for the case of the ($D^+ + D$) reactions (1a) and (1b), and the ($D^+ + H$) reaction (1c). The modified Coulomb barrier penetration factor, $P_s(E)$, is the probability of tunneling through the barrier to reach the nuclear surface. It can be computed from solutions of the Schroedinger equation for the ($D^+ + D$) system in which an attractive Coulomb potential $V_s(r)$ due to the presence of shielding electrons is included with the original repulsive Coulomb potential between two D^+ 's (two protons):

$$\left\{ -\frac{\hbar^2}{2M} \nabla^2 + V_N(r) + V_c(r) + V_s(r) \right\} \psi_{DD}(\vec{r}) = E \psi_{DD}(\vec{r}) \quad (15)$$

where $V_N(r)$ is an effective attractive nuclear potential of range $\sim 8F$ (twice the deuteron radius of $4F$) and $V_c(r)$ is the repulsive Coulomb potential between two D^+ 's,

$$V_c(r) = \frac{Z_D Z_D e^2}{r}. \quad (16)$$

The modified Coulomb barrier penetration factor, $P_s(E)$, which includes the effect of the electron screening potential $V_s(r)$ given in eq. (15) can be calculated in the Wentzel-Kramers-Brillouin (WKB) approximation as (retaining only the s-wave contribution)

$$P_s(E) = \exp\left[-2\left(\frac{2M}{\hbar^2}\right)^{1/2} \int_{r_N}^{r_a} (V_c(r) + V_s(r) - E)^{1/2} dr\right] \quad (17)$$

The effective nuclear interaction range, $r_N \approx 8F$, can be set to zero in eq. (17) without loss of accuracy. The integral in eq. (17) cannot be carried out analytically, but can be written for an attractive potential, $V_s(r) < 0$, as

$$2\left(\frac{2M}{\hbar^2}\right)^{1/2} \int_0^{r_a} (V_c(r) + V_s(r) - E)^{1/2} dr = \frac{(E_G)^{1/2}}{(E + E_s(E))^{1/2}} \quad (18)$$

where $E_s(E)$ is determined numerically as a function of E by carrying out the integral numerically for each value of $E > 0$. The modified penetration factor, $P_s(E)$, is then

$$P_s(E) = \exp(-E_G^{1/2}/(E + E_s(E))^{1/2}). \quad (19)$$

When $V_s(r) = 0$ and hence $E_s(E)$ vanishes, we recover the conventional Gamow factor, $P_s(E) = P_G(E)$. The classical turning point, r_a , in eq. (17) is determined by

$$V_c(r_a) + V_s(r_a) = E. \quad (20)$$

From eqs.(18) and (20), it can be easily shown that $E_s(E)$ in eqs.(18) and (19) is bounded by $|V_s(r_a)| < E_s(E) < |V_s(0)|$. In the following, two models for the electron screening potential $V_s(r)$ will be described.

(a) The 1s Hydrogen Electron Screening Potential.

The electron screening potential for the target D (or H) in D_2 gas (or H_2 gas) can be approximated, to reasonable accuracy, via the electron probability density $\rho_e(r)$ of the 1s hydrogen electron,

$$\rho_e(r) = -q e^{-ur}, \quad (21)$$

where $q = Z_s e / \pi a_0^3$ and $u = 2/a_0$. $Z_S, Z_D = 1$, and a_0 are the effective charge of the screening electrons, the deuteron nuclear charge, and the Bohr radius ($a_0 \approx 0.53 \text{ \AA}$), respectively. $\rho_e(r)$ is normalized such that $\int \rho_e(r) d^3r = -Z_s e$. The Coulomb potential generated by $\rho_e(r)$ as seen by an incident deuteron (D^+) is then

$$\begin{aligned} V_s(r) &= Z_D e \int \frac{\rho_e(r')}{|\vec{r} - \vec{r}'|} d^3r' \\ &= -\frac{Z_D Z_S e^2}{r} [1 - e^{-ur} (1 + ur/2)], \end{aligned} \quad (22)$$

which approaches to $-Z_D Z_S e^2/r$ as $r \rightarrow \infty$, as expected.

We note that $V_s(r)$ is negative for $r \geq 0$ and $|V_s(r)|$ has the maximum value $|V_s(0)| = Z_D Z_S e^2/a_0 = 27.17 Z_D Z_S eV$ at $r = 0$. Since $|V_s(r)|$ decreases monotonically as r increases, $E_s(E)$ is bounded by $E_s(E) \leq |V_s(0)|$. As an example, at the classical turning point of $r = r_a = a_0$ corresponding to $E = 7.35 eV$, $|V_s(a_0)| = 19.8 Z_D Z_S eV$, and hence $E_s(E)$ is bounded by $27.17 Z_D Z_S eV > E_s(E) > 19.8 Z_D Z_S eV$. It is interesting to note that for $Z_S = Z_D$, $V(r) = V_c(r) + V_s(r) = Z_D^2 e^2 (e^{-ur}/r) (1 + ur/2)$ which is similar to the Debye screening potential in condensed matter and plasma physics, $Z^2 e^2 (e^{-kr}/r)$ with $k^{-1} = r_s = (k_B T / 4\pi n_e e^2)^{1/2}$.

(b) Spherical Shell Charge Electron Screening Potential

For a simpler potential generated by a spherical shell charge distribution, $\tilde{\rho}_e(r) = (Z_s e / 4\pi r_s r_a) \delta(r - r_a)$, $V_s(r)$ can be written as

$$\tilde{V}_s(r) = -\frac{Z_D Z_S}{r_s} \Theta(r_a - r). \quad (23)$$

When $\tilde{V}_s(r)$ is used in eq. (18) the penetration factor becomes

$$\tilde{P}_s(E) = \exp(-E_G^{1/2}/(E + \tilde{E}_s)^{1/2}) \quad (24)$$

where $\tilde{E}_s = Z_D Z_S e^2 / r_s$ is a constant independent of E . Eq. (24) has been previously used for D_2 molecular fusion [10] and for analysis of D_2O cluster fusion.[13]

Using eq. (19), the new extrapolation formula appropriate for reactions (1a), (1b), (1c), and other fusion reactions is

$$\sigma_s(E) = \frac{S(E)}{E} \exp(-(E_G/(E + E_s(E)))^{1/2}). \quad (25)$$

The screening energy term $E_s(E)$ can be extracted from the measured values [16,17] of $\sigma_{exp}(E)$ for the D-D fusion reaction (1a) and be compared with the values of $E_s(E)$ given by the two models described above. The values of $E_s(E)$ extracted from $\sigma_{exp}(E < 4keV$ (CM)) [16,17] using eq. (25) are listed in Table I, and have large uncertainties. Therefore, it is important to carry out precision measurements of $\sigma_{exp}(E)$ with improved accuracies for $E < 4keV$ (CM). The experimental values of $\sigma_{exp}(E)$ [16, 17] listed in Table I are measured with D_2 gas targets for which the electron screening potential is expected to be approximately that of the 1s hydrogen electron. However, for solid targets such as T_1D and PdD, the electron screening range could be as small as a tenth of the Bohr radius, $a_0/10$, since the Debye screening length k^{-1} is $k^{-1} = r_s = (k_B T / 4\pi n_e e^2)^{1/2} \approx 0.05\text{\AA}$ with $T = 300^\circ\text{K}$ and $n_e \approx 6 \times 10^{22} \text{cm}^{-3}$. A more elaborate calculation [19] yields also $k_s \approx 0.05\text{\AA}$ at $T = 300^\circ\text{K}$ for D^+ in Pd. Therefore, the extracted values of $E_s(E)$ from the solid metal deuteride targets may be up to ten times larger than values ($E_s(E) \approx 40 - 60 \text{ eV}$) extracted from the D_2 gas target [16, 17]. Improved measurements are presently being carried out at Purdue by D. Elmore, Y.E. Kim, D.S. Koltick, E. Michlovich, and R.G. Reifenberger.

Since the precise form of $V_s(r)$ will depend on experimental and physical conditions and is not known for electrolysis experiments, it is useful to replace $E_S(E)$ of eq. (19) with an energy independent parameter \tilde{E}_s as in eq. (24) within a reasonable range of parametric values for \tilde{E}_s .

Since $E_s(E)$ in eq. (25) is expected to be of the order of $270 Z_s eV$ for the metal deuteride targets, the electron screening effect will play a very important role when $E \lesssim 270 Z_s eV$ in for electrolysis fusion experiments and for other fusion processes, as shown by a recent calculation [20] and may act in part as a catalyst of cold fusion. The electron

screening effect may explain why it is difficult to reproduce the same result with different cathode samples in electrolysis experiments and may also explain why the reported tritium production [7,8] lasts only for a finite period in electrolysis experiments, since the fusion rate and cross section are very sensitive to variation of flux and kinetic energies of D^+ and also to the electron density and screening potential around D in the cathode surface layer, which may be difficult to maintain and could be different for each electrolysis experiment due to the a non-equilibrium situation and other experimental conditions. The extracted values of $E_s(E)$ from $\sigma_{exp}(E)$ using eq. (25) should enable us to determine an effective electron screening potential and also the corresponding electron density surrounding the deuterium nucleus in the metal surface layer.

V. MUON SCREENING EFFECT

The screening effect is expected to be substantially larger for a muonic atomic or molecular target, since the muonic Bohr radius, a_0^μ , is much smaller than a_0 , $a_0^\mu \approx a_0/196 \approx 2.7 \times 10^{-3} \text{\AA}$ for D ($a_0^\mu \approx a_0/186$ for H) and thus $|V_s^\mu(0)| \approx 196|V_s(0)| \approx 5318 \text{ eV}$ (5054 eV for H) for $Z_S = Z_D$. In order to study the muonic screening effect on fusion reactions, the fusion cross-sections should be measured as a function of energy using a muonic atom (or molecule) beam and/or target for reactions, (1a), (1b), and (1c). This expected large increase of the muonic deuterium fusion rate brings up an interesting possibility that a minute amount of the background muonic hydrogen or deuterium atoms, produced by cosmic rays and present in electrolysis experiments might participate in fusion reactions that compete with or dominate over the regular fusion reactions (1a), (1b), and (1c).

For the muon screening effect on reactions (1a) and (1b), order of magnitude estimates for the fusion rates can be made with reasonable accuracy using eq. (11) for the rate $\Lambda_s^\mu(E)$ with a sharp velocity distribution. This is because the values of $E_s(E) > |V_s^\mu(r_a)|$ are substantial larger than the corresponding values of $E < 0.1 \text{ keV}$. For the 1s hydrogen muon screening potential $V_s^\mu(r)$, the Bohr radius a_0 in eq. (22) is replaced by the muonic Bohr radius a_0^μ . Assuming that $E_s(E) = |V_s^\mu(r_a)|$ (which is an underestimate), the fusion rate, $\Lambda_s^\mu(E) = n_D^\mu \sigma(E) v(\text{CM})$, for the sum of the two reactions (1a) and (1b) is calculated at several values of $E(\text{CM})$ and summarized in table II.

As can be seen from table II, the observed rates of $\Lambda_{exp}^n(1b) \approx 10^{-23} \text{ sec}^{-1}/D$ [4] and $\Lambda_{exp}^T(1a) \approx 10^{-19} \text{ sec}^{-1}/D$ [3] can be explained if very small densities of $n_D^\mu \approx 10^3$ and 10^7 cm^{-3} , respectively, are

assumed (in D_2O or PdD), using Λ_f^μ ($E = 2.1$ eV) $\approx n_D^\mu (3.9 \times 10^{-26} \text{ cm}^3/\text{sec})$. However, it is difficult to maintain the background density of $n_D^\mu \approx 10^3 \sim 10^7 \text{ cm}^{-3}$ from the cosmic ray muons (produced by pions, neutrino, etc.) [21]. Nevertheless, it is useful to study the muon screening effect for reactions (1a), (1b), and (1c) by carrying out two types of experiments: (a) scattering experiments in which a muonic atom (or molecule) beam or target is used, and (b) electrolysis experiments exposed to muon (or pion) beam from an accelerator. This later type of experiment should be examined as a possible prototype for a practical fusion reactor.

VI. BRANCHING RATIO FOR THE D-D FUSION REACTIONS

The suppression of reaction (1b) and the enhancement of reaction (1a) at low energies have been observed in electrolysis experiments [3,7,8] contrary to the conventional assumption of nearly equal rates based on the charge symmetry and the charge independence of the nuclear force.

After the incident deuteron penetrates through the Coulomb barrier within an effective nuclear interaction range of $8F$ (twice the deuteron radius), nuclear dynamics take over for this system of four nucleons. One possible explanation for the unequal rates is that there may be a broad resonance behavior in $\sigma(E)$ for reaction (1a) but not in $\sigma(E)$ for reaction (1b) at low energies, which is plausible since the final state Coulomb interaction is present for reaction (1a) but not for reaction (1b). If $\sigma(E)$ happens to have resonance behavior near $E \approx 0$, the extrapolation may yield erroneous values for $\sigma(E \approx 0)$, since the non-resonant relation (2) is not applicable to resonance reactions. Therefore, it is very important to investigate the possibility of resonance behavior for $\sigma(E)$ near $E \approx 0$ theoretically, and also to measure $\sigma(E \approx 0)$ directly with precision experiments. Recent observation of neutron bursts at -30°C at a rate of $\Lambda \approx 10^{-23} \text{ sec}^{-1}$ reported by Menlove et al. [22] may be interpreted as the existence of a sharp resonance in the reaction channel (1b).

At present, there are neither direct experimental measurements nor theoretical calculations of the branching ratios for reactions (1a) and (1b) for $E \lesssim 3 \text{ keV}$. One would expect the branching ratio of reaction (1a) to be larger than that of reaction (1b), since reaction (1b) involves a fusion of two protons to form ^3He while reaction (1a) does not fuse two protons but merely transfers a neutron from one deuteron to another to form ^3H . Theoretical calculations of the reaction cross-sections and branching ratios of reactions (1a) and (1b) should be carried

out based on non-relativistic four-nucleon scattering theory [23] using nucleon-nucleon forces and the Coulomb interaction.

VII. SUMMARY

It has been shown that the effect of electron screening may be essential in describing the electrolysis fusion experiments and other related physical processes. When combined with the effect of velocity distribution in the context of the surface reaction mechanism, the screening effect may be able to explain the claimed values of $\Lambda_{exp}^T(1a) \approx 10^{-19}/D$ [3] and $\Lambda_{exp}^n(1b) \approx 10^{-23} \text{ sec}^{-1}/D$ [4]. The effects of velocity distribution and electron screening may also be able to explain the claimed value of $\Lambda_{exp}^{heat} \approx 10^{-10} \text{ sec}^{-1}/D$ [3].

It is important to improve the accuracy of the measurements of the cross section for reaction (1a) below 4 keV (LAB) in order to determine the magnitude of the electron screening effect on the Coulomb barrier penetration factor and fusion rates. It is suggested that the screening effect should be investigated with metal deuteride targets and also with a muonic atom (or molecule) beam and/or target for reactions (1a), (1b), and (1c), since the screening effect is then expected to be substantially larger. The electron screening effect may provide a plausible explanation for the results of the electrolysis experiments and also for other physical processes [24] such as the earth's internal heating [4] and the excess heat radiation from other outer planets [24].

The observed suppression [3,7,8] of the branching ratio for reaction (1b) is expected to be due to nuclear resonance and dynamic effects which involve the attractive short-range nuclear forces among four nucleons (two neutrons and two protons) and the Coulomb repulsive barrier between the fusing protons within the range of $1.6F$ (twice proton radius) to $8F$ (twice the deuteron radius). These effects will modify the $S(E)$ factor in eq. (25).

ACKNOWLEDGEMENT

The author wishes to thank Gary S. Chulick and Robert A. Rice for helpful discussion and suggestions.

REFERENCES

1. Y.E. Kim, "Nuclear Theory Hypotheses for Cold Fusion", to be published in the Proceedings of the NSF/EPRI Workshop on Anomalous Effects in Deuterated Metals, Washington, D.C., October 16-18, 1989.

2. Y.E. Kim, "Fission-induced inertial confinement hot fusion and cold fusion with electrolysis", to be published in LASER INTERACTION AND RELATED PLASMA PHENOMENA, Volume 9 (H. Hora and G.H. Miley eds.).
3. M. Fleischmann and S. Pons, "Electrochemically Induced Nuclear Fusion" J. of Electroanal. Chem., **261**, 301 (1989); and errata, **263**, 187 (1989).
4. S.E. Jones et al., "Observation of Cold Nuclear Fusion in Condensed Matter", Nature **338**, 737 (27 April 1989).
5. A.J. Appleby, S. Srinivasan, Y.J. Kim, O.J. Murphy, and C.R. Martin, "Evidence for Excess Heat Generation Rates During Electrolysis of D_2O in LiOD using a Palladium Cathode - a Microcalorimetric Study", in the Proceedings of the Workshop on Cold Fusion Phenomena, May 23-25, 1989, Santa Fe, New Mexico, to be published in J. Fusion Energy, March 1990.
6. A. Belzner, U. Bischler, G. Crouch-Baker, T.M. Gur, G. Lucier, M. Schreiber, and R. Huggins "Two Fast Mixed-conductor Systems: Deuterium and Hydrogen in Palladium-Thermal Measurements and Experimental Considerations", in the Proceedings of the Workshop on Cold Fusion Phenomena, May 23-25, 1989, Santa Fe, New Mexico, to be published in J. Fusion Energy, March 1990.
7. K.L. Wolf, N.J.C. Packham, D.R. Lawson, J. Shoemaker, F. Cheng, and J.C. Wass, "Neutron Emission and the Tritium Content Associated with Deuterium Loaded Palladium and Titanium Metals", in the Proceedings of the Workshop on Cold Fusion Phenomena, May 23-25, 1989, Santa Fe, New Mexico, to be published in J. Fusion Energy, March 1990.
8. P.K. Iyengar, "Cold Fusion Results in BARC Experiment", in the Proceedings of the 5th International Conference on Emerging Nuclear Energy Systems (ICENES V), Karlsruhe, West Germany, July 3-6, 1989.
9. A.J. Leggett and G. Baym, "Exact Upper Bound on Barrier Penetration Probabilities in Many-Body Systems: Application to Cold Fusion", Phys. Rev. Lett. **63**, 191 (1989).
10. K. Langanke, H.J. Assenbaum, and C. Rolfs, "Screening Corrections in Cold Deuterium Fusion Rates", Z. Phys. A. Atomic Nuclei **333**, 317 (1989).
11. R.A. Rice, G.S. Chulick, Y.E. Kim, and J.-H. Yoon, "The Role of Velocity Distribution in Cold Deuterium-Deuterium Fusion", Purdue Nuclear Theory Group Report PNTG-90-5 (January 1990), submitted to Fusion Technology.
12. Y.E. Kim, "Cross-Section for Cold Deuterium-Deuterium Fusion", to be published in Fusion Technology, May, 1990.
13. M. Rabinowitz and D.H. Worledge, "An Analysis of Cold and Lukewarm Fusion", to be published in Fusion Technology **17**, (1990).
14. Y.E. Kim, R.A. Rice, and G.S. Chulick, "The Role of the Proton-Deuterium Fusion Cross Section in Physical Processes", PNTG-90-7 (February 1990), submitted to Fusion Technology.
15. W.A. Fowler, G.R. Caughlan, and B.A. Zimmermann, "Thermonuclear Reaction Rates", Ann. Rev. Astr. Astrophys. **5**, 525 (1967); "Thermonuclear Reaction Rates II", **13**, 69 (1975).
16. A. von Engel and C.C. Goodyear, "Fusion Cross-Section Measurements with Deuterons of Low Energies", Proc. Roy. Soc. A **264**, 445 (1961).
17. A. Krauss, H.W. Becker, H.P. Trautvetter, and C. Rolfs, "Low-Energy Fusion Cross Sections of D+D and D + 3He Reactions", A**465**, 150 (1987).
18. H.H. Anderson and J.F. Ziegler, "Hydrogen Stopping Powers and Ranges in All Elements", Pergamon Press, New York (1977).
19. S. N. Vaidya and Y. S. Mayya, "Theory of Screening-Enhanced D-D Fusion in Metals", Jap. J. of Appl. Phys. **28**, L2258 (1989).
20. R.A. Rice, G. S. Chulick, and Y. E. Kim, "The Effect of Velocity Distribution and Electron Screening on Cold Fusion", to be published in the Proceedings of the First Annual Conference on Cold Fusion, Salt Lake City, Utah, March 28-31, 1990.
21. S. Hayakawa, *Cosmic Ray Physics*, Wiley, New York (1969).
22. H. O. Menlove et al., "The Measurements of Neutron Emissions from Ti Plus D_2 Gas", in the Proceedings of Workshop on Cold Fusion Phenomena, May 23-25, 1989, Santa Fe, New Mexico, to be published in J. Fusion Energy.

23. O. A. Yakubovsky, *Yad. Fiz.* **5** 1312 (1967) [*Sov. J. Nucl. Phys.* **5**, 937 (1967)]; P. Grassberger and W. Sandhas, *Nucl. Phys.* **B2**, 181 (1967); E. O. Alt, P. Grassberger and W. Sandhas, *J.I.N.R. Report No. E4-6688* (1971).

24. Y. E. Kim, R. A. Rice, and G. S. Chulick, "The Electron Screening Effect on Fusion Cross-Sections and Rates in Physical Processes", *Purdue Nuclear Theory Group Report PNTG-90-9* (March, 1990).

Table I

Extracted values of the electron screening parameter, $E_s(E)$, for eq. (25) from the experimental values of the D-D fusion cross section, $\sigma_{\text{exp}}(E)$, for reaction (1a), $D(D^+, p)^3H$, at low energies, $E < 4\text{keV}$ (CM). $\sigma_{\text{calc}}(E)$ is calculated with the conventional extrapolation formula, eq.(2), with $S(E) = 52.9\text{keV} - b$ and $E_G^{1/2} = 31.39(\text{keV})^{1/2}$. The superscripts a and b in the first column refer to references 16 and 17, respectively.

E (keV in CM)	$\sigma_{\text{exp}}(E)$ (barn)	$\sigma_{\text{calc}}(E)$ (barn)	$E_s(E)$ (eV)
2.0 ^a	$(8.4 \pm 4.6) \times 10^{-9}$	6.06×10^{-9}	$59 \pm \begin{smallmatrix} 79 \\ 143 \end{smallmatrix}$
2.98 ^b	$(2.54 \pm 0.37) \times 10^{-7}$	2.25×10^{-7}	$40 \pm \begin{smallmatrix} 46 \\ 52 \end{smallmatrix}$
3.98 ^b	$(2.19 \pm 0.13) \times 10^{-6}$	1.95×10^{-6}	$58 \pm \begin{smallmatrix} 30 \\ 32 \end{smallmatrix}$

Table II

The fusion rate, $\sigma(E) v(\text{CM})$, for reactions (1a) and (1b), $D(D^+, p)^3H$ and $D(D^+, n)^3He$, calculated from eq. (25) with the muon screening energy term $E_s(E) = |V_s^\mu(r_a)|$. The classical turning point r_a is in units of the muonic Bohr radius $a_o^\mu \approx a_o/186 \approx 2.85 \times 10^{-3} \text{ \AA}$.

E (eV)	r_a (a_o^μ)	$ V_s^\mu(r_a) $ (keV)	$\sigma(E)$ (b)	$\sigma(E) v(\text{CM})$ (cm^3/sec)
0.036	6	0.844	2.1×10^{-9}	5.6×10^{-28}
0.276	5	1.01	5.4×10^{-9}	3.9×10^{-27}
2.12	4	1.26	1.9×10^{-8}	3.9×10^{-26}
16.7	3	1.67	1.0×10^{-7}	5.8×10^{-25}